Liquid crystal modulator with ultra-wide dynamic range and adjustable driving voltage

Xing-jun Wang,[1] Zhang-di Huang,[1] Jing Feng,[1] Xiang-fei Chen,[1] Xiao Liang,[2] and Yan-qing Lu[1*]

[1] *Department of Materials Science and Engineering and National Laboratory of Solid State Microstructures, Nanjing University, Nanjing 210093, P. R. China*
[2] *Department of Chemistry, Tsinghua University, Beijing 100084, P. R. China*
* Corresponding author: *yqlu@nju.edu.cn*

Abstract: We demonstrated a reflective-type liquid crystal (LC) intensity modulator in 1550 nm telecomm band. An effective way to compensate the residual phase of a LC cell is proposed. With the adjustment of a true zero-order quarter wave plate and enhanced by total internal reflection induced birefringence, over 53 dB dynamic range was achieved, which is much desired for some high-end optical communication, infrared scene projection applications. In addition, the driving voltages were decreased and adjustable. Mechanical and spectral tolerance measurements show that our LC modulator is quite stable. Further applications of our experimental setup were discussed including bio-sensors and high speed modulators.

OCIS codes: (230.3720) Liquid-crystal devices; (060.2340) Fiber optics components

References and links

1. D. K. Yang and S. T. Wu, *Fundamentals of Liquid Crystal Devices* (John Wiley & Sons, England, 2006), Chap. 12.
2. R. James, F. A. Fernández, S. E. Day, M. Komarcevic, and W. A. Crossland, "Modelling of the diffraction efficiency and polarization sensitivity for a liquid crystal 2-D spatial light modulator for reconfigurable beam steering," J. Opt. Soc. Am. **24**, 2464–2473 (2007).
3. W. Dickson, G. A. Wurtz, P. R. Evans, R. J. Pollard, A. V. Zayats, "Electronically controlled surface plasmon dispersion and optical transmission through metallic hole arrays using liquid crystal, " Nano Lett. **8**, 281-286 (2008)
4. S. Manzanera, P. M. Prieto, D. B. Ayala, J. M. Lindacher, and P. Artal, "Liquid crystal Adaptive Optics Visual Simulator: Application to testing and design of ophthalmic optical elements," Opt. Express **15**, 16177-16188 (2007).
A. G. Maksimochkin, S. V. Pasechnik, V. A. Tsvetkov, D. A. Yakovlev, G. I. Maksimochkin and V. G. Chigrinov, "Electrically controlled switching of light beams in the plane of liquid crystal layer," Opt. Commun. **270**, 273-279 (2007).
5. C. Mao, M. Xu, W. Feng, T. Huang, K. Wu, and J. Wu, "Liquid-crystal applications in optical telecommunication," Proc. SPIE **5003,** 121-129 (2003).
6. X. Liang, Y. Q. Lu, Y. H. Wu, F. Du, H. Y. Wang and S. T. Wu, "Dual-frequency addressed variable optical attenuator with submillisecond response time," Jpn. J. App. Phys. **44**, 1292-1295 (2005).
7. Y. H. Wu, Y. H. Lin, Y. Q. Lu, H. Ren, Y. H. Fan, J. R. Wu and S. T. Wu, "Submillisecond response variable optical attenuator based on sheared polymer network liquid crystal," Opt. Express, **12**, 6377-6384 (2004).
8. J. L. West, G. Zhang, and A. Glushchenko, "Fast birefringent mode stressed liquid crystal," Appl. Phys. Lett. **86**, 031111 (2005).
9. S. Jutamulia, G. M. Storti, W. M. Seiderman, J. Lindmayer and D. A. Gregory, "Infrared signal processing using a liquid crystal television," Opt. Eng. **30**, 178-182 (1991).
10. C. Chen, P. J. Bos, J. Kim, Q. Li and J. E. Anderson, "Improved liquid crystals for vertical alignment applications," J. Appl. Phys. **99**, 123523 (2006)
11. M. Born and E. Wolf, *Principles of Optics*, 7th edition (Cambridge U., Cambridge, UK, 1999), Chap. 1.

#96030 - $15.00 USD Received 9 May 2008; revised 22 Jun 2008; accepted 23 Jun 2008; published 13 Aug 2008

1. Background and motivation

In addition to the well-known flat panel displays and projectors, liquid crystal (LC) has also been widely used in many tunable photonic devices, such as spatial light modulators, tunable lenses, optical phase arrays, variable optical attenuators (VOAs), and optical switches. [1-6]. In comparison with the competing micro-electro mechanical systems (MEMS) technology, LC devices exhibit some advantages, e.g., no-moving-parts, low power consumption, high reliability and low cost in small volume [6]. A major drawback of the LC based photonic devices is their relatively slow response, which is more severe in infrared band as the cell gap is thicker. Up to date, a lot of approaches have been demonstrated to overcome this problem, including dual-frequency addressing [7], high voltage overdriving, and polymer-network introduction. [8, 9] Besides response time, dynamic range, *i.e.*, the on-off states' contrast ratio is another key figure of merit for displays and photonic LC devices. For example, a fiber optic attenuator needs wide dynamic range to supply a pure off-state for wavelength blocking and network protection. Additionally, a LC on silicon based infrared scene projection with ultra-wide dynamic range is also rather desirable. [10] Therefore low background scenes to high bright radiance objects, such as missile plume, could be well displayed for scene simulation in Hardware-in-the-loop systems.

For MEMS technology, light is mechanically deflected thus high contrast ratio is relatively easy to achieve; while with regard to a LC device, which is normally based on polarization manipulation. Both the polarizer quality and accurate polarization control should be satisfied simultaneously. However, for ordinary LC devices with homogeneous alignment, there is residual phase retardation even at a high driving voltage, as LC molecules may not be realigned due to surface anchoring. Even the LC alignment layer itself may exhibit small birefringence. Figure 1 shows the measured phase retardation at 1550 nm of a 3.8 μm homogeneously aligned cell filled with Merck 6647 LC. Even with the driving voltage over $15V_{rms}$, there is still remarkable residual phase that will affect the most achievable dark state. Although vertical alignment (VA) is a good solution for wide dynamic range in normally-off devices, [11] the cost and material availability are potential concerns especially in the infrared band. Actually even the VA cell still has slight initial phase retardation due to the LC pretilt angle. To solve this problem, some companies use oblique dielectric birefringent coatings to compensate the residual phase. Complicated process control thus has to be adopted. As a consequence, a simple approach to cancel the residual phase effect is very desirable.

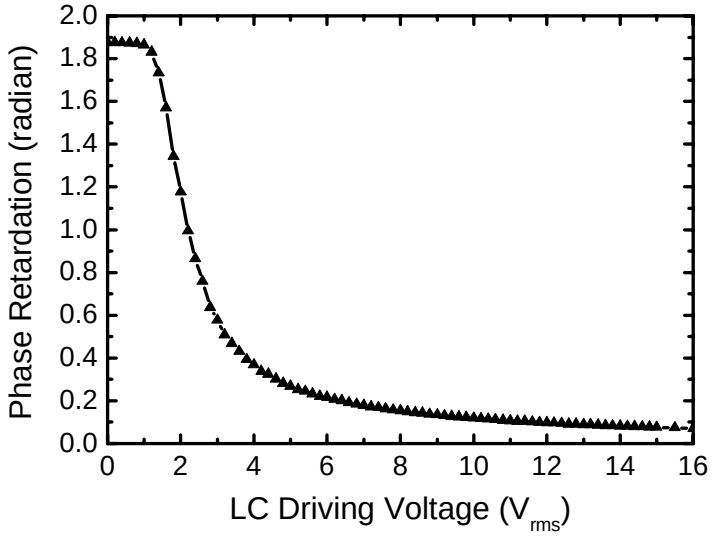

Fig. 1. Phase retardation of a LC cell showing residual phase effect.

#96030 - $15.00 USD Received 9 May 2008; revised 22 Jun 2008; accepted 23 Jun 2008; published 13 Aug 2008

In this work, we designed a compact reflective LC intensity modulator at 1550 nm telecomm wavelength band. A true zero-order quarter wave plate (QWP) was inserted in the light path with well designed orientation angle. We demonstrated that an over 53 dB dynamic range may be achieved with wide spectral tolerance range. Another merit is that the driving voltage becomes adjustable at any given attenuation state. For example, the corresponding voltage for 20 dB attenuation could drop to less than half of its original voltage without phase compensation. Factors that affect the device performances were studied. We found that our setup and compensation technique are also very suitable for some other applications like bio-sensoring and high speed electro-optic modulating.

2. Experimental setup and results

Figure 2 depicts the schematic diagram of our optical design where the ray tracing is modeled by the optical simulation software Zemax™. A polarization beam displacer (PBD) and a homogeneously-aligned, 45°-rubbed LC cell are sandwiched between an input fiber collimator and a silica retro-reflector. The LC cell is just what we used for phase measurement in Fig. 1. A quartz true zero-order QWP is placed between the PBD and LC cell. To study the residual phase compensation effect, the QWP was removed at the beginning for comparison. Light from the input fiber is collimated by a collimator with 70-mm working distance. When the light comes into the PBD, which is a 10 mm long, 45° cut birefringent crystal Calcite, the light is separated into an ordinary beam and an extraordinary beam, respectively. Only the part of light whose polarization states are rotated by 90° can be recombined by the PBD and then coupled back into the fiber, which is the "on" state of the modulator. In this case, the combination of QWP, LC and retro-reflector together should act like a half wave plate (HWP). When a sufficiently high electric field is applied to the LC cell, the original phase retardation of the cell is disrupted. In an ideal "off" state, the beams' polarizations retain their original states after passing through the QWP, LC, retro-reflector, LC and then QWP again. Thus the two returned beams are further separated by the PBD. As a result, no light is coupled back into the collimator. Arbitrary attenuation levels could be achieved by controlling the applied AC voltage.

As the input and output port share the same fiber, a circulator is used for light power measurement. In our experiments, all elements except for the retro-reflector have anti-reflection coating around 1550 nm. To further suppress back reflection, all elements should be tilted by a small angle which is not illustrated in the diagram.

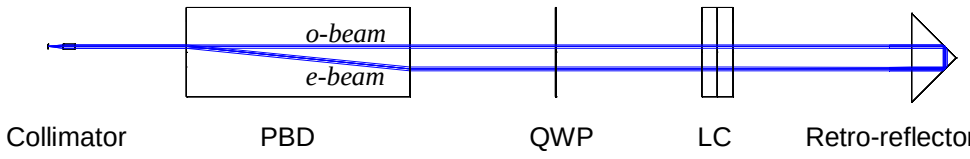

Fig. 2. A LC based light intensity modulator design with Zemax™ optical simulation software.

To characterize the performance of our LC-based intensity modulator, a HP 8168E tunable laser working at λ=1550 nm was used as the light source, whose polarization state was randomly controlled by manually adjusting the optical fiber. As both the extraordinary and ordinary beams pass the same route in opposite directions, all polarization dependant issues like polarization dependant loss and polarization mode dispersion are self-cancelled. This phenomenon was proven in our experiments. To obtain a low attenuation on-state when there is no voltage applied, the initial phase of the LC cell should be close to a quarter wave (π/2) so that we can get ~π phase after doubly passing the cell. In our experiments, the cell is just what we used for the phase measurement as shown in Fig. 1. The reason why we selected a

#96030 - $15.00 USD Received 9 May 2008; revised 22 Jun 2008; accepted 23 Jun 2008; published 13 Aug 2008

slight thicker cell is to make sure the lowest attenuation state at π total phase retardation could be identified, which is the reference level of our attenuation measurements.

Figure 3 illustrates the voltage-dependent transmittance by recording the attenuations while adjusting the driving voltage. At first, the QWP was not employed. The result is shown as the top curve. The symbols are the measurement points. From the curve, the optical threshold voltage is 0.8 V_{rms}. As the applied voltage increases, the curve shows a small bumper to its lowest attenuation. Then the transmittance decreases continuously with voltage increasing. However, the maximum attenuation at 15 V_{rms} only reaches 23 dB, which agrees well with the measured phase retardation in Fig. 1. It is clear that the residual phase contributes to the low dynamic range.

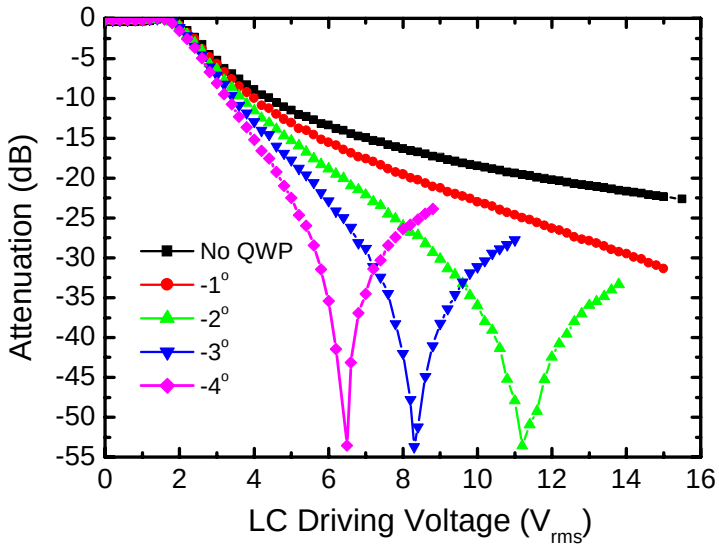

Fig. 3. Voltage-dependent transmittance of a LC based intensity modulator at different QWP rotation angles, where the top curve is for no-QWP and the others from top to bottom corresponds to -1°, -2°, -3° and -4° QWP rotation angles, respectively.

According to our optical design, a QWP was inserted between the PBD and LC cell. Its orientation could be adjusted as the QWP is attached on a rotational stage. The rotation angle is defined as the angle between QWP's fast-axis and the extraordinary beam's polarization direction. If the rotational angle is zero, the QWP's fast axis is just at the same plane of PBD's optical axis. In this case, the transmittance curve shows no change before and after the QWP is placed, which is exhibited in Fig. 3 with the top curve. Then we gradually rotated the QWP and measured the transmittance again. In this case, the QWP would involve in the total phase retardation. As we know, in a transmissive mounting, a QWP may convert any elliptical polarization to linear polarization, but a successive HWP should be used to further tune the polarization angle so that a pure dark state could be achieved. However, our case is a reflective type as it suits the current trend of small footprint devices. Light passes through the cell twice. Adjusting the QWP, the polarization state revolution becomes more complicated and difficult to analyze in a straightforward way. It is interesting to see how the QWP affects polarizations. With the help of Jones matrix calculus, we investigated the polarization state change at each step. Taking the QWP orientation angle as a variable, we found that there is really a solution where the whole elements together acts like a HWP, which corresponds to a high attenuation state. The second top curve in Fig. 3 corresponds to a QWP orientation angle at -1°. The attenuation is enhanced evidently: the 15 V_{rms} attenuation reaches -31dB which is already close to low-end telecomm standard. After we adjusted the QWP angle to -2°, a -53.6

#96030 - $15.00 USD Received 9 May 2008; revised 22 Jun 2008; accepted 23 Jun 2008; published 13 Aug 2008

dB (~200,000: 1) ultra-high attenuation was achieved, and the corresponding driving voltage was 11.2V_{rms}. Further rotating the QWP to -3° and -4°, over 53 dB dynamic ranges still could be obtained with decreasing voltages. For example, the driving voltage for -20 dB attenuation drops to less than 5V, only 2/5 of the original value without the QWP. This is a very useful feature as we are able to select a suitable QWP angle and voltage combination to get a low driving voltage and wanted attenuation slope.

As a light modulator, the tolerances are very critical for practical applications. We studied the angular tolerance and spectral response of the above setup. Figure 4 shows the attenuation as a function of the QWP's orientation angle. We set the QWP at -2°, -3° and -4° then adjusted the voltage to reach their maximum attenuations. For example, when the QWP orientates at -2°, the voltage at highest attenuation (-53.6 dB) is 11.2 V_{rms}. If we fix the voltage at 11.2 V_{rms} and then rotate the QWP angle gradually, the angular tolerance is thus obtained as shown in Fig. 4. All these 3 curves show similar trends: the attenuation weakens when the QWP angle has an offset. The tolerance bandwidth at 40 dB is about 0.5° for all three voltages. The 30 dB bandwidths are wider than 1.6°. We believe these tolerances are quite acceptable for current mechanical positioning and optical packaging techniques. The spectral response of our light intensity modulator was also carefully studied as described in Fig. 5. We measured the modulator performance at the whole telecomm wavelength C band (1530 nm – 1570 nm), which is quite flat. The whole band attenuation flatness at -10 dB, -20 dB and -30 dB are 0.2 dB, 0.4 dB and 1.2 dB, respectively. When the attenuation further increases to -40 dB and -50 dB, the fluctuation goes severe. This might result from our sample quality, mechanical movement, voltage stability and noises, among which, the circulator's crosstalk between the input and returning output port might be a key factor. If the circulator could be saved by using a dual-collimator design, better spectral flatness at high attenuation states and higher dynamic range can be reasonably expected. However, the optical design showing in Fig. 2 should be modified for that purpose. As lights from one collimator generate two beam spots on LC cell, a dual-collimator design might give rise to four light spots on the cell. Better LC cell uniformity will be required in that situation.

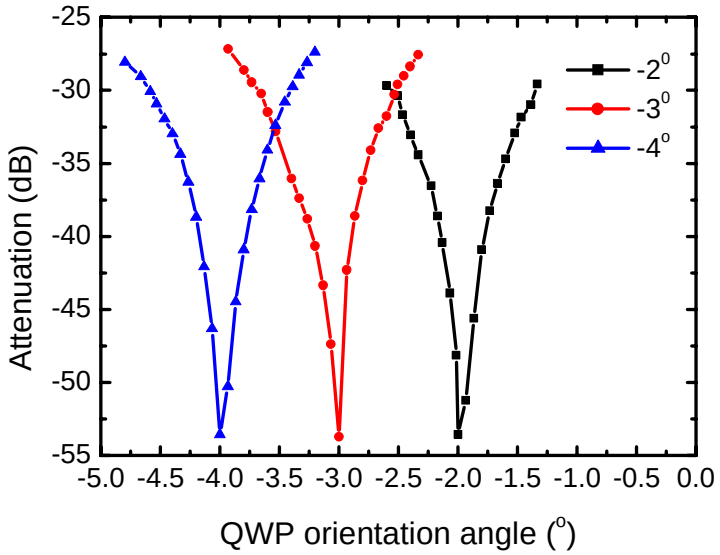

Fig. 4. QWP angular tolerance curves corresponding to different driving voltages. (11.2 V_{rms}, 8.3 V_{rms}, 6.5 V_{rms}, respectively).

#96030 - $15.00 USD Received 9 May 2008; revised 22 Jun 2008; accepted 23 Jun 2008; published 13 Aug 2008

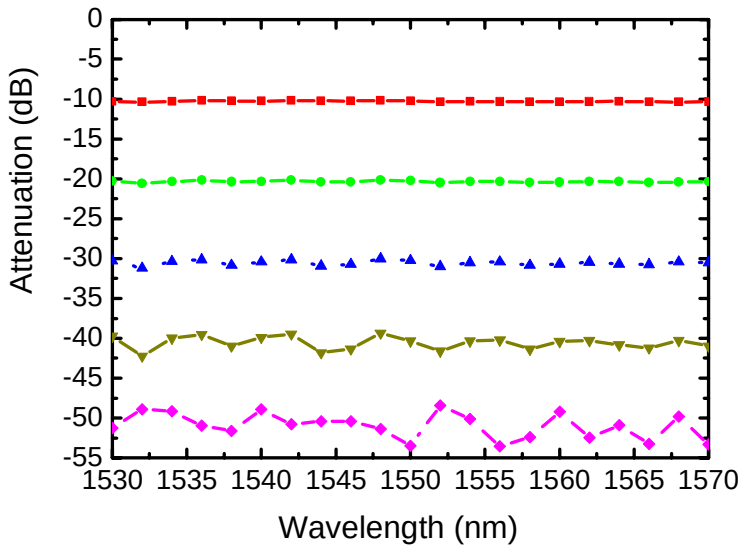

Fig. 5. Spectral response at telecomm C-band of a LC based intensity modulator. Different curves correspond to different attenuations states.

3. Analysis and discussions

From our experimental results above, we demonstrated that a single well-placed QWP may totally compensate a LC cell's residual phase. An over 50 dB ultra-wide dynamic range was achieved. This approach could be employed together with fast-response LC technique like dual frequency addressing and voltage over driving to improve the overall device performances. [7] However, when we tried to correlate the experimental results (discrete symbols in Fig. 6) and theoretical simulation (dash line in Fig. 6) at -2° QWP orientation, an apparent difference between them was found. The highest attenuation should occur at >16 V_{rms} according to simulation based on the measured LC phase retardation in Fig. 1; while the actual attenuation maximum is far from it at 11.2 V_{rms}. Further analysis reveals that the phase retardation induced by total internal reflection (TIR) in the retro-reflector should be taken into account. Deduced from the well known Fresnel equations, there is a phase change at TIR surface, while phase shifts are different for s and p polarizations as shown in Eq. (1). [12]

$$\begin{cases} \varphi_s = 2\tan^{-1}\dfrac{\sqrt{\sin^2\theta - 1/n^2}}{\cos\theta} \\ \varphi_p = 2\tan^{-1}\dfrac{\sqrt{\sin^2\theta - 1/n^2}}{\cos\theta/n^2} \end{cases} \tag{1}$$

where θ is the incident angle and n is the refractive index of retro-reflector glass. With the increase of glass index, the phase difference between s and p waves becomes larger, leading to a remarkable TIR induced birefringence. In our case, the retro-reflector is made with Silica. Its index at 1550 nm is 1.444. The TIR critical angle is thus 43.8°. In our experiment, the lights hit the back-surfaces of retro-reflector at 45°, which is larger than the critical angle. Both the s and p waves are totally reflected. However, their phase shifts at the TIR surface are calculated to be 0.4 radian and 0.8 radian, respectively, according to Eq. (1). As the s and p waves correspond to the ordinary beam and extraordinary beam inside the PBD, one TIR surface thus could be treated as a 0.8-0.4=0.4 radian phase plate with its optical axis oriented

#96030 - $15.00 USD Received 9 May 2008; revised 22 Jun 2008; accepted 23 Jun 2008; published 13 Aug 2008

at 0°. As a consequence, the LC modulator's transmittance were modulated. With consideration of the TIR birefringence, we recalculated the transmittance as shown in Fig. 6 with a solid line curve. Now it agrees well with the experimental results. In another word, the calculated TIR birefringence is proven. As we know, the TIR relies on environmental index, and any index change will affect TIR birefringence. Our setup thus gives rise to a unique way to study TIR and monitor environmental refractive index change. A novel index measurement equipment or bio-sensor with no moving parts thus might be developed based on this architecture. As our system is sensitive around the maximum attenuation voltages, any small birefringence change will induce large transmittance variation. We may also apply this idea to study elasto-optical effect and design new high-speed low-voltage electro-optic modulators. Some of these works are now on the way.

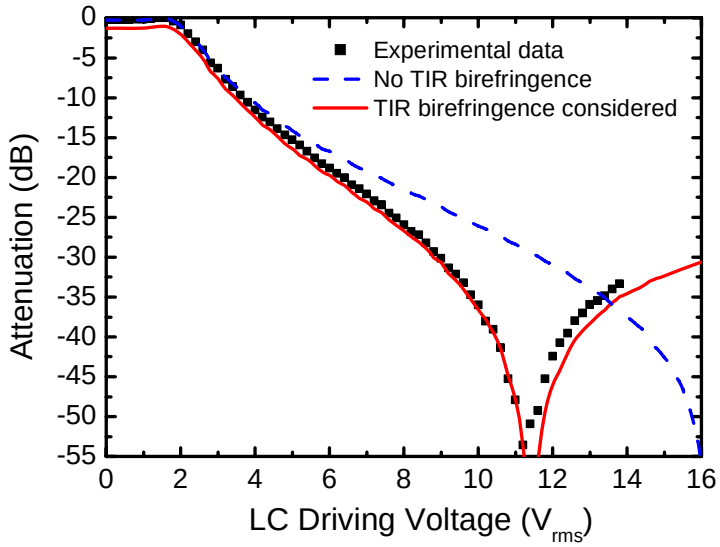

Fig. 6. Correlation of theoretical and experimental results, with and without consideration of total internal reflection induced birefringence.

4. Conclusion

We demonstrated a LC based light intensity modulator with an over 50 dB dynamic range. A compact reflective type optical architecture was employed to suppress the polarization dependant issues. The mechanism to reach such a high dynamic range was discussed. A well-placed true zero-order QWP is able to cancel the LC cell's residual phase, while the TIR induced birefringence also plays an important role. It doesn't compensate the phase residual by itself while it may enhance the QWP's effect. With the adjustment of the QWP's orientation angle, the LC cell's driving voltage also could decrease dramatically. Some potential applications of our LC modulator are discussed, which might be both fundamentally interesting and practically useful.

Acknowledgments

We thank EZconn Corporation and Dr. Hui-tian Wang's technical supports. This work was sponsored by China 863 program under contract No. 2006AA03Z417 and quantum modulation program under contract No. 2006CB921805. Yan-qing Lu acknowledges the support from China MOE for new century and Changjiang scholars program.

#96030 - $15.00 USD Received 9 May 2008; revised 22 Jun 2008; accepted 23 Jun 2008; published 13 Aug 2008